Journal of Nuclear Medicine, published on January 27, 2022 as doi:10.2967/jnumed.121.263289

Positron emission tomography imaging of system x_C^- in immune cells for assessment of disease activity in mice and patients with inflammatory bowel disease

Short title: Imaging of inflammatory bowel disease

Minjung Seo[1*], Yeji Kim[2*], Byong Duk Ye[3*], Sang Hyoung Park[3], Seog-Young Kim[2], Jin Hwa Jung[2], Sung Wook Hwang[3], Sun Young Chae[4], Dong Yun Lee[4], Sang Ju Lee[4], Seung Jun Oh[4], Jihun Kim[5], Ji Young Kim[6], Sae Jung Na[7], Misung Kim[8], Sang-Yeob Kim[2], Norman Koglin[9], Andrew W. Stephens[9], Mi-Na Kweon[2], Dae Hyuk Moon[4]

[1]Department of Nuclear Medicine, Ulsan University Hospital, University of Ulsan College of Medicine, Ulsan, Republic of Korea.

Departments of [2]Convergence Medicine, [3]Gastroenterology, [4]Nuclear Medicine, and [5]Pathology, Asan Medical Center, University of Ulsan College of Medicine, Seoul, Republic of Korea.

[6]Department of Nuclear Medicine, Hanyang University Medical Center, Hanyang University College of Medicine, Seoul, Republic of Korea.

[7]Department of Radiology, Uijeongbu St. Mary's Hospital, College of Medicine, The Catholic University of Korea, Seoul, Republic of Korea.

[8]Department of Pathology, Ulsan University Hospital, Ulsan, Republic of Korea.

[9]Life Molecular Imaging GmbH, Berlin, Germany.

*Contributed equally to this work. They are not under training.

Dae Hyuk Moon, MD.: dhmoon@amc.seoul.kr; 82-2-3010-4592; 0000-0001-9892-4276

Mi-Na Kweon, PhD.: mnkweon@amc.seoul.kr; 82-2-3010-2096; 0000-0003-2916-2524

88, Olympic-ro 43-gil, Songpa-gu, Seoul 05505, Republic of Korea

Word count: 4963

We aimed to explore whether the imaging of antiporter system x_C^- of immune cells with (4*S*)-4-(3-^{18}F-fluoropropyl)-L-glutamate (^{18}F-FSPG) positron emission tomography (PET) can assess inflammatory bowel disease (IBD) activity in murine models and patients (NCT03546868). **Methods:** ^{18}F-FSPG PET imaging was performed to assess IBD activity in mice with dextran sulfate sodium-induced and adoptive T-cell transfer-induced IBD and a cohort of 20 patients at a tertiary care center in South Korea. Immunohistochemical analysis of system x_C^- and cell surface markers was also studied. **Results:** Mice with experimental IBD showed increased intestinal ^{18}F-FSPG uptake and xCT expression in $CD11c^+$, $F4/80^+$, and $CD3^+$ cells in the lamina propria, increases positively associated with clinical and pathological disease activity. ^{18}F-FSPG PET studies in patients, most of whom were clinically in remission or had mildly active IBD, showed that PET imaging was sufficiently accurate in diagnosing endoscopically active IBD and remission in patients and bowel segments. ^{18}F-FSPG PET correctly identified all nine patients with superficial or deep ulcers. Quantitative intestinal ^{18}F-FSPG uptake was strongly associated with endoscopic indices of IBD activity. The number of $CD68^+xCT^+$ and $CD3^+xCT^+$ cells in 22 bowel segments from patients with ulcerative colitis and the number of $CD68^+xCT^+$ cells in seven bowel segments from patients with Crohn's disease showed a significant positive association with endoscopic indices of IBD activity. **Conclusion:** The assessment of system x_C^- in immune cells may provide diagnostic information on the immune responses responsible for chronic active inflammation in IBD. ^{18}F-FSPG PET imaging of system x_C^- activity may noninvasively assess the IBD activity.

Keywords: system x_C^-; immune cells; positron emission tomography; inflammatory bowel disease

Inflammatory bowel disease (IBD) consists of two types of chronic incurable intestinal disorders, ulcerative colitis (UC) and Crohn's disease (CD). Tight monitoring of disease activity is essential throughout the course of the disease to guide therapeutic decisions and assess response to therapy and relapse (*1,2*). Although endoscopic mucosal healing is a long-term goal of therapy, endoscopic evaluation may not always be feasible due to lack of immediate availability, cost, need for bowel preparation, relatively poor patient acceptance, and complications. Less invasive markers of disease activity are therefore needed.

Key immune processes involved in the pathogenesis of IBD include cytokine production by activated dendritic cells and macrophages, and the development of effector T lymphocyte subsets (*3*). Targeting dysfunctional immune cells and their products has led to the development of new therapies that have benefited patients (*3*). Similarly, a noninvasive method that targets dysfunctional immune cells, distinguishing between active cell subsets and quiescent cell populations, may allow specific assessment of disease activity, rather than relying on nonspecific indicators of disease activity (*4*).

System x_C^- plays an important role in the regulation of the innate and adaptive immune systems (*5*), and upregulated in activated macrophages (*6,7*). Upon antigen stimulation, proliferating T cells require sufficient glutathione levels to ensure proper reactive oxygen species balance, resulting in the induction of high levels of xCT for cystine uptake (*8,9*). An *ex vivo* study in patients with IBD has shown that intestinal lamina propria macrophages expressed xCT, which resulted in high glutathione levels and full T-cell receptor reactivity (*10*). All these results suggest that system x_C^- could be a specific indicator of disease activity in IBD. Researches designed to characterize the functional relevance of system x_C^- in disease state with oxidative stress and inflammation might pave the way for diagnosing and treating IBD (*5*).

(4S)-4-(3-^{18}F-fluoropropyl)-L-glutamate (^{18}F-FSPG) is a ^{18}F-labeled L-glutamate derivative that is

specifically taken up by system x_C^- (*11*). An exploratory clinical study has shown that ^{18}F -FSPG positron emission tomography (PET) can detect inflammation of the lungs and sarcoidosis (*12*). The low background uptake of ^{18}F-FSPG would be especially advantageous in detecting inflammatory lesions in the intestine (*12,13*), an organ in which the utilization of conventional ^{18}F-fluorodeoxyglucose imaging may be limited because of physiologic uptake. ^{18}F-fluorodeoxyglucose PET may also be limited in differentiating mildly active IBD from endoscopic remission (*14,15*), showing an adequate accuracy only for detecting moderate-to-severe endoscopic disease (*16,17*). The objective of this study was to evaluate whether the *in vivo* assessment of system x_C^- in immune cells provides information on the dysregulated immune responses responsible for chronic active inflammation in IBD, thereby assessing the disease activity. We first conducted animal experiments to investigate whether ^{18}F-FSPG would have increased accumulation associated with xCT expression in immune cells. Second, we aimed to explore the diagnostic validity of ^{18}F-FSPG PET/computed tomography (CT) in patients. Finally, we assessed the association of ^{18}F-FSPG uptake and xCT expression in immune cells with endoscopic markers.

MATERIALS AND METHODS

Experimental IBD Models, ^{18}F-FSPG PET Imaging, and Ex Vivo Analysis

The research protocol was approved by the Institutional Animal Care and Use Committee (Registration Numbers: 2016-12-153 and 2017-12-017). All animal experiments conformed to the institutional guidelines. Experimental details are reported in accordance with the ARRIVE guidelines 2.0. Dextran sulfate sodium (DSS)-induced and adoptive T-cell transfer-induced IBD models were evaluated. Details of clinical disease activity, *ex vivo* analysis and immunohistochemical staining for expression of xCT and cell surface markers are provided in the Supplemental Methods.

Clinical Study Design and Patients

This was a prospective, non-randomized, single-center cohort study. The study protocol, provided in the supplemental materials, was approved by the Ministry of Food and Drug Safety of the Republic of Korea and the institutional review board of Asan Medical Center (2018-0262). This trial was conducted in accordance with the Declaration of Helsinki and institutional guidelines. All patients provided written informed consent before participation. The primary objective was to explore the validity of ^{18}F -FSPG PET/CT for the diagnosis of patients with active IBD. The secondary objectives were to explore the validity of ^{18}F-FSPG PET/CT for detecting bowel segments with active IBD, to assess the correlation of ^{18}F-FSPG activity with clinical, endoscopic, and biological markers of disease activity, to assess the inter-reader variability of visual ^{18}F-FSPG PET/CT interpretation, and to evaluate the safety of ^{18}F-FSPG PET/CT. Intended enrollment included 10 patients with UC and 10 with CD, numbers regarded as sufficient to obtain PET/CT imaging information while avoiding unnecessary exposure to ionizing radiation. The trial was registered at http://clinicaltrials.gov as NCT03546868.

Patients eligible for inclusion were consecutive adults aged between 19 and 79 years who had UC or CD, as diagnosed clinically, endoscopically, and histologically. The complete inclusion and exclusion criteria are listed in Supplemental Methods. All patients were identified based on presenting symptoms, as evaluated by three of the authors (BDY, SHP, and SWH) at the Department of Gastroenterology.

^{18}F-FSPG PET/CT Imaging of Patients

Patients were asked to fast for at least 4 hours before administering ^{18}F-FSPG (8 hours if they were on a high protein diet). A dose of 200 ± 20 MBq ^{18}F-FSPG was administered as a slow intravenous bolus injection for up to 60 seconds. Sixty minutes later, PET/CT was performed from the abdomen to the pelvis, with an acquisition time of 3 minutes per bed, using a PET/CT scanner (Discovery PET/CT 690, GE

Healthcare, Milwaukee, WI, USA). The total radiation exposure from the CT examination did not exceed 1 mSv. Hyoscine butylbromide was administered intravenously before or during the PET/CT to reduce peristaltic movement. For the safety assessment of ^{18}F-FSPG, see Supplemental Methods.

Images were interpreted independently by two board-certified nuclear medicine physicians who were blinded to clinical and endoscopic data. ^{18}F-FSPG intensity moderately higher compared with the liver was considered positive for active disease. The maximum SUV (SUVmax) of each bowel segment was also determined, with the summed SUVmax being the sum of all segments. Disagreements between the two physicians were resolved by consensus. Details are provided in Supplemental Methods (*12,13*).

Assessment of Disease Activity

Endoscopic assessment was considered a valid reference standard for disease activity and the extent. Sigmoidoscopy or colonoscopy was performed by an experienced gastroenterologist (BDY, SHP, or SWH) blinded to ^{18}F-FSPG PET/CT results. The severity and extent of inflammatory lesions were evaluated using the Ulcerative Colitis Endoscopic Index of Severity (UCEIS) in UC patients and the Crohn's Disease Endoscopic Activity Index of Severity (CDEIS) in CD patients (*18*). Segmental scores were determined in five bowel segments per patient using the UCEIS or CDEIS. For segmental CDEIS, the score for ulcerated or non-ulcerated stenosis was imputed to the affected segment. Endoscopic evidence of active UC was defined as a UCEIS score ≥2, whereas endoscopic evidence of active CD was defined as a CDEIS score ≥3. Bowel segments with a superficial or deep ulcer were considered a severe disease. Clinical and pathological assessment are summarized as Supplemental Methods (*18*).

Immunohistochemical Staining of Human xCT, GLUT1, and Cell Surface Markers

The immunohistochemistry study was approved by the institutional review board of Asan Medical Center

(2019-0260). Written informed consent was obtained again from all participants. The details are summarized in Supplemental Methods (*19*) and Supplemental Table 1.

Statistical Analysis

The sensitivity of ^{18}F-FSPG PET/CT for the diagnosis of patients with endoscopic evidence of active disease was calculated as the probability of positive ^{18}F-FSPG uptake in patients with active disease, as defined by the UCEIS or CDEIS. Specificity was defined as the probability of negative ^{18}F-FSPG uptake when the disease was not present. Bowel segment-level sensitivity and specificity were determined according to segmental UCEIS and CDEIS scores. Bowel segments that were not assessed by endoscopy were excluded from the analysis. The details are provided in Supplemental Methods.

RESULTS

In vivo Animal Studies

Twelve of fifteen DSS-treated mice and 11 of 15 mice that underwent adoptive T-cell transfer met the eligibility criteria and completed the study. The control groups consisted of six and ten mice, respectively. Clinical disease activity of DSS-treated mice on day 7 (median, 1.8; range, 0.7–3.3) and T-cell–transferred mice 8–12 weeks after transfer (median, 2.5; range, 1.0–4.0) was significantly higher than that of their respective control groups ($P < 0.001$; Supplemental Figure 1).

In DSS-treated mice, an increased ^{18}F-FSPG uptake in the colon was observed (Figure 1). The SUVmax of ^{18}F-FSPG was significantly higher in the colons of DSS-treated than control mice (median, 2.1 [range, 0.5–3.9] vs. 0.7 [range, 0.5–1.9], $P = 0.018$), as was the pathologic score derived from colon tissue (median, 14.2 [range, 5.8–32.0] vs. 1.5 [range, 0–2.8]; $P < 0.001$). The SUVmax of ^{18}F-FSPG uptake was positively associated with clinical disease activity ($\rho = 0.57$, $P = 0.014$) and pathologic scores ($\rho =$

0.65, $P = 0.004$; Figure 1 and Supplemental Figure 2).

Similarly, the SUVmax of colonic ^{18}F-FSPG uptake (median, 4.5 [range, 2.9–6.8] vs. 0.7 [range, 0.5–0.9], $P < 0.001$) and the pathologic score derived from colon tissue (median, 8.3 [range, 6.4–14.8] vs. 0.8 [range, 0.4–1.6], $P < 0.001$) were significantly higher in T-cell transferred than in control mice (Figure 2). The SUVmax of ^{18}F-FSPG uptake showed positive associations with clinical disease activity ($\rho = 0.74$, $P < 0.001$) and pathologic scores ($\rho = 0.74$, $P < 0.001$; Figure 2 and Supplemental Figure 3).

Immunohistochemical staining of colon tissues revealed that xCT and GLUT1 were highly expressed in CD11c$^+$ dendritic cells, F4/80$^+$ macrophages, and CD3$^+$ T cells in the lamina propria from mice with experimental colitis (Supplemental Figure 4). In addition, immunohistochemical staining showed that xCT and GLUT1 were expressed in the epithelial cells of normal and inflamed mucosa.

Patients and ^{18}F-FSPG PET/CT Procedure

Between August 2018 and January 2019, 23 patients with IBD were assessed for initial eligibility and invited to participate in this prospective study. Three patients withdrew their consent before the injection of ^{18}F-FSPG. Finally, ten patients with UC and ten with CD were enrolled. All 20 patients completed ^{18}F-FSPG PET/CT as planned. The median administered activity per patient was 199.8 MBq (range, 192.4–214.6 MBq), and the median administered mass dose was 0.82 μg (range, 0.21–1.86 μg). Nineteen patients underwent colonoscopy, and one underwent sigmoidoscopy 1 day after ^{18}F-FSPG PET/CT. The demographic and baseline clinical characteristics are listed in Table 1. Six patients with UC (60%) and eight with CD (80%) showed endoscopic evidence of active disease. Twelve (26%) of 47 bowel segments in patients with UC and 24 (59%) of 41 segments in patients with CD showed active inflammatory lesions.

^{18}F-FSPG Uptake in Patients

Readers determined that overall image quality was adequate for interpretation in all patients. The inter-reader agreements of visual assessment of ^{18}F-FSPG accumulation were kappa values of 0.70 (95% CI, 0.49–0.92) for patient-level analysis and 0.65 (95% CI, 0.57–0.73) for bowel segment-level analysis. Two readers disagreed on the presence of ^{18}F-FSPG accumulation in 2 (10%) of 20 patients and 10 (11%) of 95 bowels segments.

^{18}F-FSPG PET/CT was positive in four (67%) of the six UC patients with endoscopically active inflammation (Figure 3) and correctly diagnosed endoscopic remission in two (50%) of the four patients (Supplemental Table 2). The two false-negative patients had scores of 3 (Supplemental Figure 5), and the two false-positives had scores of 4 (Supplemental Figure 6). The sensitivity and specificity of ^{18}F-FSPG PET/CT in identifying active bowel segments were 75% (9/12) and 86% (30/35), respectively. All patients (n = 2) and bowel segments (n = 5) with superficial or deep ulcers were correctly identified.

All eight CD patients with active inflammation (Figure 4) and two with endoscopic remission were correctly diagnosed by ^{18}F-FSPG PET/CT (Supplemental Table 3). In a segment-based analysis, ^{18}F-FSPG PET/CT had a sensitivity of 71% (17/24) and a specificity of 94% (16/17), respectively. All seven patients and 16 of 20 segments with superficial or deep ulcerations were correctly diagnosed.

Association between ^{18}F-FSPG Uptake and Disease Activity

In patients with UC, the median SUVmax was 3.1 (range, 1.8–8.2). The summed SUVmax was strongly associated with the UCEIS ($\rho = 0.79$, $P = 0.006$) but not with the partial Mayo score, C-reactive protein, and fecal calprotectin (Supplemental Figure 7). The segmental SUVmax (median, 2.2; range, 0.8–8.2) also showed strong associations with UCEIS (n = 47, $\rho = 0.66$, $P < 0.001$) and the Robarts Histopathological Index (n = 23, $\rho = 0.64$, $P = 0.001$).

The median SUVmax in patients with CD was 5.6 (range, 2.8–7.6). The summed SUVmax was strongly associated with the Crohn's Disease Activity Index, C-reactive protein, fecal calprotectin, and the CDEIS (Supplemental Figure 8). The segmental SUVmax (median, 2.9; range, 1.5–7.6) also showed a strong association with CDEIS (n = 41, $\rho = 0.61$, $P < 0.001$) but not with the Colonic and Ileal Global Histologic Disease Activity Score (n = 7, $\rho = 0.33$, $P = 0.47$).

Safety of ^{18}F-FSPG PET/CT

No adverse events were observed in patients with UC. However, four patients (40%) with CD had adverse events with mild intensity, including diarrhea, upper respiratory infection, arthritis, and dizziness. None of adverse events was related to the study drug, and none of patients experienced any serious adverse events or any clinically relevant changes in safety parameters.

Association between xCT Expression and Disease Activity

Immunohistochemical staining showed that $CD68^+$, $CD3^+$, or $CD66b^+$ cells were present in the lamina propria of intestinal mucosa affected by UC (Supplemental Figure 9) or CD (Supplemental Figure 10). In addition, xCT was found to be expressed in the inflammatory and epithelial cells of all bowel segments. In patients with UC, the numbers of $CD68^+xCT^+$, $CD3^+xCT^+$, and $CD66b^+xCT^-$ cells in 22 bowel segments showed positive associations with UCEIS and SUVmax (Supplemental Table 4). By contrast, $cytokeratin^+xCT^+$ was negatively associated with UCEIS and SUV. In patients with CD, only the number of $CD68^+xCT^+$ cells in seven bowel segments showed a significant association with CDEIS (Supplemental Table 5). Other cell populations showed no association with CDEIS or SUV.

DISCUSSION

Using mice with experimental IBD, we found that ^{18}F-FSPG accumulation in the colon was associated with disease activity indices and xCT expression in immune cells. Expansion of this study to patients, most of whom were clinically in remission or had mildly active IBD, showed that ^{18}F-FSPG PET/CT was accurate in diagnosing endoscopically active IBD and remission in patients and bowel segments. All patients with superficial or deep ulcers were correctly identified. Quantitative ^{18}F-FSPG uptake and xCT expression in immune cells were associated with endoscopic disease activity indices. ^{18}F-FSPG PET/CT was well tolerated with no study drug-related adverse events. Our results suggest that ^{18}F-FSPG PET/CT can assess disease activity and distinguish between active IBD and mucosal healing, as determined endoscopically.

Although this study did not include participants across the entire range of disease activity, the subjects of this study may constitute a representative sample of those that would likely be the intended use population for ^{18}F-FSPG PET/CT. All patients were evaluated by endoscopy after ^{18}F-FSPG PET/CT, with blinded readers interpreting ^{18}F-FSPG PET/CT. Thus, there are no potential risks of bias and applicability regarding the accuracy of data. False-positives and false-negatives were likely due to an indeterminate zone for decision-making. Greater experience with refined classification criteria may reduce the likelihood of patient misclassification. The positive association between quantitative ^{18}F-FSPG uptake and endoscopic assessment further supports the validity of ^{18}F-FSPG PET/CT. In patients with UC, the absence of a significant association between ^{18}F-FSPG uptake and conventional markers may be due to the inclusion of patients with mildly active disease and the small study sample.

We found that endoscopic assessment was positively associated with xCT expression by $CD68^+$ and $CD3^+$ immune cells in patients with UC and with xCT expression by $CD68^+$ cells in CD, but not with xCT^+CD66b^+ cells. Although the small number of assessed bowel segments with CD may have precluded

a consistent association, these results confirm the role of $CD68^+xCT^+$ macrophages in the antioxidative microenvironment of IBD (*10*). Our results also demonstrate that xCT expression is upregulated in human $CD3^+$ T cells, further strengthening the evidence for xCT expression and cystine uptake as regulators of T-cell function. These findings are consistent with results showing high initial rates of cystine and ^{18}F-FSPG uptake followed by decreases during a later phase of inflammation (*6,11,12*). xCT expression and cystine uptake in immune cells might mirror cellular concentrations of reactive oxygen species as well as metabolic activity (*20*). Taken together, these findings suggest that *in vivo* ^{18}F-FSPG PET/CT results may indicate broad changes in immune metabolism. Understanding of xCT in immune cells may also provide a pathological tool to assess IBD activity.

Interestingly, the endoscopic assessment was negatively associated with xCT expression by $cytokeratin^+$ cells in patients with UC. xCT was expressed on the apical surfaces of the epithelial cells (Supplemental Figures 9 and 10), where absorption occurs (*10,21*). This localization to absorptive sites suggests that system x_C^- plays a role in intestinal cystine transport (*21*) but does not involve ^{18}F-FSPG transport into the epithelial cells. The reason for this lack of association between $GLUT1^+$ immune cells and endoscopic assessment is not apparent but may be related to the persistent glucose hypermetabolism in healing tissue after inflammation (*22,23*).

Radiation exposure is an important limitation in using ^{18}F-FSPG PET/CT to assess disease activity, mainly because most of these patients are relatively young. Current guidelines recommend using cross-sectional imaging modalities that do not entail exposure to ionizing radiation when it is likely that serial examinations are required (*1*). A per patient dose of 200 MBq ^{18}F-FSPG would result in a mean effective dose of 4.0 ± 0.2 mSv, including the dose from CT (*24*). These doses can be significantly reduced by using high sensitive PET/CT systems (*25*). Study protocols that allow a low dose of ^{18}F-FSPG can reduce radiation dose as much as 75% without clinical detriment (*26*).

This study had several limitations. First, the diagnostic validity should be interpreted with caution because of the small number of included patients and the exploratory nature of the present study. Additional studies in larger numbers of patients are required to validate our initial results. Second, the assessment of IBD activity was based on endoscopic findings. Thus, comparisons between endoscopy and ^{18}F-FSPG PET/CT may be limited because the actual sites of endoscopic evaluation may not precisely match those of ^{18}F-FSPG uptake, thereby underestimating the accuracy of ^{18}F-FSPG PET/CT for evaluating bowel segments.

CONCLUSION

^{18}F-FSPG PET/CT imaging of system x_C^- in immune cells can noninvasively assess IBD activity and remission of the entire bowel without the need for bowel preparation and safety issues related to invasive endoscopic procedures. Assessment of system x_C^- expression by immune cells may provide diagnostic information on the dysregulated immune responses responsible for chronic active inflammation.

DISCLOSURE

This research was sponsored by Asan Foundation (Seoul, Republic of Korea) and financially supported by National Research Foundation grants funded by the Korea Ministry of Science and ICT, Republic of Korea (grant numbers: NRF-2016M2A2A7A03913219 and NRF-2019R1A2C209022213), and the Korea Health Technology R&D Project through the Korea Health Industry Development Institute, funded by the Ministry of Health & Welfare, Republic of Korea (grant number: HI18C2383). The funders had no role in the conceptualization or design of the study; in the collection, analysis, and interpretation of the data; in the writing of the manuscript; or in the decision to submit the manuscript for publication. NK and AWS report personal fees from Life Molecular Imaging GmbH (employment) during the conduct of the study

and are listed as coinventors on a patent application entitled "[F-18]-labeled L-glutamic acid and L-glutamine derivatives (I), their use and processes for their preparation; US 9,308,282", which is owned by Life Molecular Imaging. DHM reports receiving grants from the National Research Foundation of Korea, the Korea Health Industry Development Institute, and Life Molecular Imaging GmbH. The other authors declare no competing interests.

KEY POINTS

QUESTION: Does *in vivo* assessment of system x_C^- in immune cells provide information on the dysregulated immune responses responsible for chronic active inflammation in inflammatory bowel disease, thereby assessing the disease activity?

PERTINENT FINDINGS: System x_C^- expression in immune cells was associated with endoscopic disease activity indices. Positron emission tomography imaging of system x_C^- was accurate in diagnosing endoscopically active disease and remission in patients and bowel segments

IMPLICATIONS FOR PATIENT CARE: Positron emission tomography imaging of system x_C^- may noninvasively assess disease activity and remission without the need for bowel preparation and safety issues related to endoscopic procedures.

REFERENCES

1. Lichtenstein GR, Loftus EV, Isaacs KL, Regueiro MD, Gerson LB, Sands BE. ACG clinical guideline: management of Crohn's disease in adults. *Am J Gastroenterol.* 2018;113:481-517.

2. Rubin DT, Ananthakrishnan AN, Siegel CA, Sauer BG, Long MD. ACG clinical guideline: ulcerative colitis in adults. *Am J Gastroenterol.* 2019;114:384-413.

3. de Souza HS, Fiocchi C. Immunopathogenesis of IBD: current state of the art. *Nat Rev Gastroenterol Hepatol.* 2016;13:13-27.

4. Dearling JL, Daka A, Veiga N, Peer D, Packard AB. Colitis immunoPET: defining target cell populations and optimizing pharmacokinetics. *Inflamm Bowel Dis.* 2016;22:529-538.

5. Lewerenz J, Hewett SJ, Huang Y, et al. The cystine/glutamate antiporter system x(c)(-) in health and disease: from molecular mechanisms to novel therapeutic opportunities. *Antioxid Redox Signal.* 2013;18:522-555.

6. Sato H, Fujiwara K, Sagara J, Bannai S. Induction of cystine transport activity in mouse peritoneal macrophages by bacterial lipopolysaccharide. *Biochem J.* 1995;310 (Pt 2):547-551.

7. Nabeyama A, Kurita A, Asano K, et al. xCT deficiency accelerates chemically induced tumorigenesis. *Proc Natl Acad Sci U S A.* 2010;107:6436-6441.

8. Garg SK, Yan Z, Vitvitsky V, Banerjee R. Differential dependence on cysteine from transsulfuration versus transport during T cell activation. *Antioxid Redox Signal.* 2011;15:39-47.

9. Levring TB, Hansen AK, Nielsen BL, et al. Activated human CD4+ T cells express transporters for both cysteine and cystine. *Sci Rep.* 2012;2:266.

10. Sido B, Lasitschka F, Giese T, et al. A prominent role for mucosal cystine/cysteine metabolism in intestinal immunoregulation. *Gastroenterology.* 2008;134:179-191.

11. Koglin N, Mueller A, Berndt M, et al. Specific PET imaging of xC- transporter activity using a (1)(8)F-labeled glutamate derivative reveals a dominant pathway in tumor metabolism. *Clin Cancer Res.* 2011;17:6000-6011.

12. Chae SY, Choi CM, Shim TS, et al. Exploratory clinical investigation of (4S)-4-(3-18F-fluoropropyl)-L-glutamate PET of inflammatory and infectious lesions. *J Nucl Med.* 2016;57:67-69.

13. Baek S, Mueller A, Lim YS, et al. (4S)-4-(3-18F-fluoropropyl)-L-glutamate for imaging of xC transporter activity in hepatocellular carcinoma using PET: preclinical and exploratory clinical studies. *J Nucl Med.* 2013;54:117-123.

14. Li Y, Beiderwellen K, Nensa F, et al. [(18)F]FDG PET/MR enterography for the assessment of inflammatory activity in Crohn's disease: comparison of different MRI and PET parameters. *Eur J Nucl Med Mol Imaging.* 2018;45:1382-1393.

15. Tenhami M, Virtanen J, Kauhanen S, et al. The value of combined positron emission tomography/magnetic resonance imaging to diagnose inflammatory bowel disease: a prospective study. *Acta Radiol.* 2021;62:851-857.

16. Shih IL, Wei SC, Yen RF, et al. PET/MRI for evaluating subclinical inflammation of ulcerative colitis. *J Magn Reson Imaging.* 2018;47:737-745.

17. Li Y, Khamou M, Schaarschmidt BM, et al. Comparison of (18)F-FDG PET-MR and fecal biomarkers in the assessment of disease activity in patients with ulcerative colitis. *Br J Radiol.* 2020;93:20200167.

18. Walsh AJ, Bryant RV, Travis SP. Current best practice for disease activity assessment in IBD. *Nat Rev Gastroenterol Hepatol.* 2016;13:567-579.

19. Ahn J, Jin M, Song E, et al. Immune profiling of advanced thyroid cancers using fluorescent multiplex immunohistochemistry. *Thyroid.* 2021;31:61-67.

20. Siska PJ, Kim B, Ji X, et al. Fluorescence-based measurement of cystine uptake through xCT shows requirement for ROS detoxification in activated lymphocytes. *J Immunol Methods.* 2016;438:51-58.

21. Burdo J, Dargusch R, Schubert D. Distribution of the cystine/glutamate antiporter system xc- in the brain, kidney, and duodenum. *J Histochem Cytochem.* 2006;54:549-557.

22. Lazzeri E, Bozzao A, Cataldo MA, et al. Joint EANM/ESNR and ESCMID-endorsed consensus document for the diagnosis of spine infection (spondylodiscitis) in adults. *Eur J Nucl Med Mol Imaging.* 2019;46:2464-2487.

23. Priftakis D, Riaz S, Zumla A, Bomanji J. Towards more accurate (18)F-fluorodeoxyglucose positron emission tomography ((18)F-FDG PET) imaging in active and latent tuberculosis. *Int J Infect Dis.* 2020;92S:S85-S90.

24. Smolarz K, Krause BJ, Graner FP, et al. (S)-4-(3-18F-fluoropropyl)-L-glutamic acid: an 18F-labeled tumor-specific probe for PET/CT imaging--dosimetry. *J Nucl Med.* 2013;54:861-866.

25. Surti S, Viswanath V, Daube-Witherspoon ME, Conti M, Casey ME, Karp JS. Benefit of improved performance with state-of-the art digital PET/CT for lesion detection in oncology. *J Nucl Med.* 2020;61:1684-1690.

26. Alberts I, Sachpekidis C, Prenosil G, et al. Digital PET/CT allows for shorter acquisition protocols or reduced radiopharmaceutical dose in [(18)F]-FDG PET/CT. *Ann Nucl Med.* 2021;35:485-492.

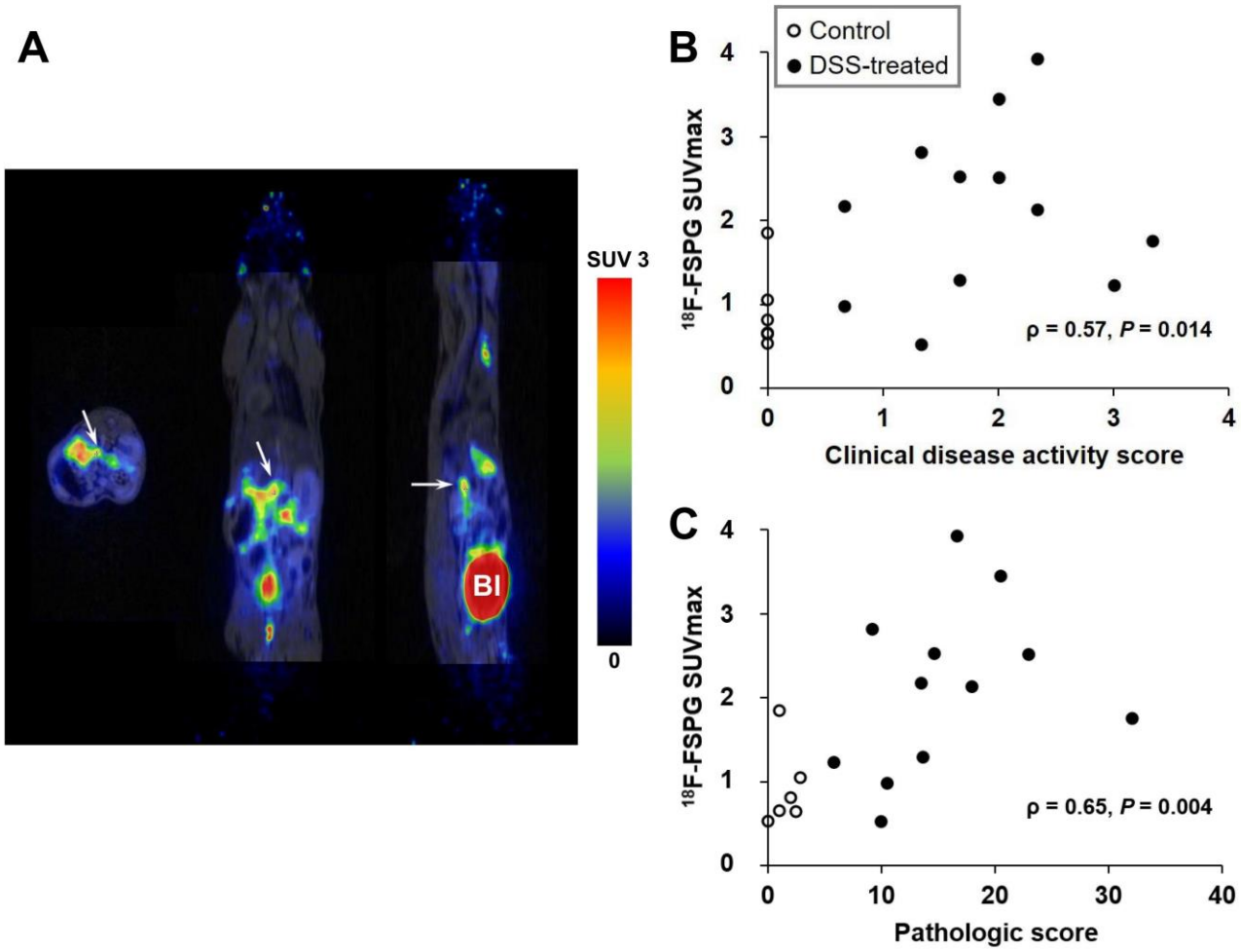

FIGURE 1. ^{18}F-FSPG imaging in DSS-treated mice. (A) Representative transaxial, coronal, and sagittal ^{18}F-FSPG PET/MRI images of the murine DSS-induced IBD model. Arrows indicate positive ^{18}F-FSPG uptake along the colon. (B, C) Associations of colonic SUVmax with (B) clinical disease activity and (C) pathologic score. Bl, bladder.

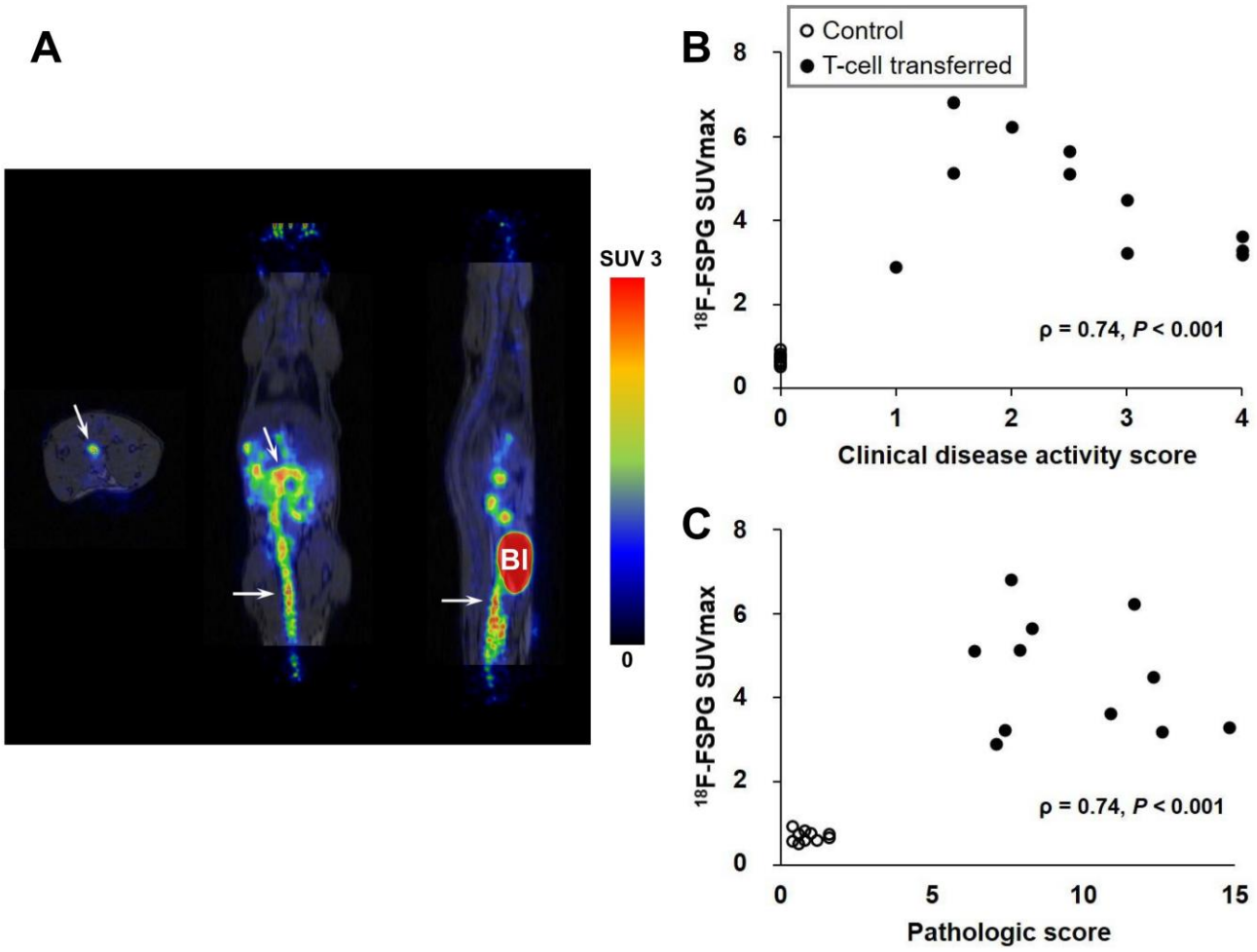

FIGURE 2. ^{18}F-FSPG imaging in T-cell transferred mice. (A) Representative transaxial, coronal, and sagittal ^{18}F-FSPG PET/MRI images of the T-cell transfer-induced IBD model. Arrows indicate increased ^{18}F-FSPG uptake in the colon. (B, C) Associations of colonic SUVmax with (B) clinical disease activity and (C) pathologic score. Bl, bladder.

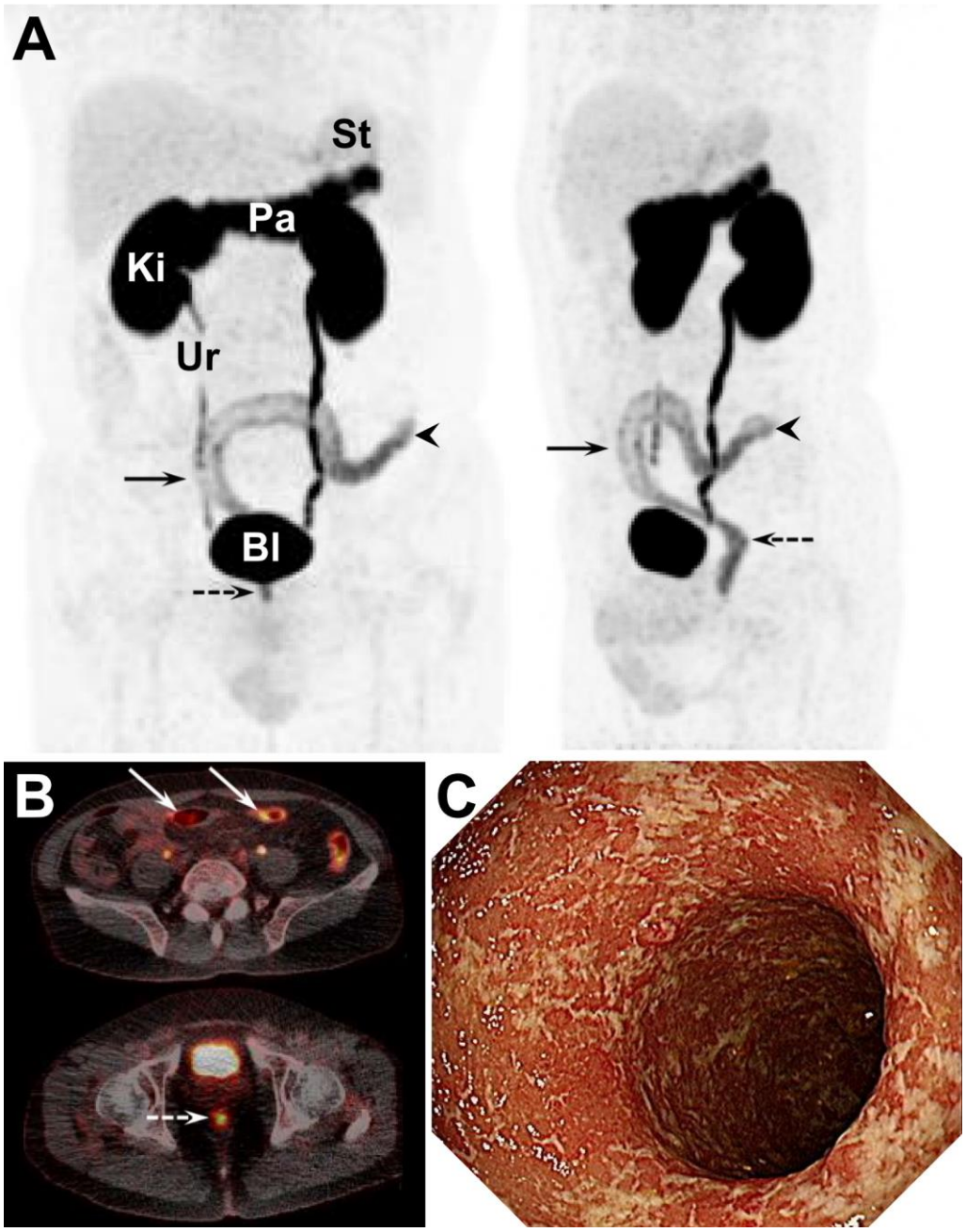

FIGURE 3. ^{18}F-FSPG PET/CT and endoscopic images of a 55-year-old man with UC presented with increased stool frequency, loose stools, hematochezia, and mild leukocytosis. His partial Mayo score was 4. (A) Maximum intensity projection and (B) axial ^{18}F-FSPG PET show increased ^{18}F-FSPG uptake along the distal descending colon (arrowhead), sigmoid colon (arrow), and rectum (dotted arrow) with endoscopically active inflammation. The segmental UCEIS of the ascending and transverse colon was 0, and that of the descending colon (C), sigmoid colon, and rectum was 5. St, stomach; Pa, pancreas; Ki, kidneys; Ur, ureter; and Bl, bladder.

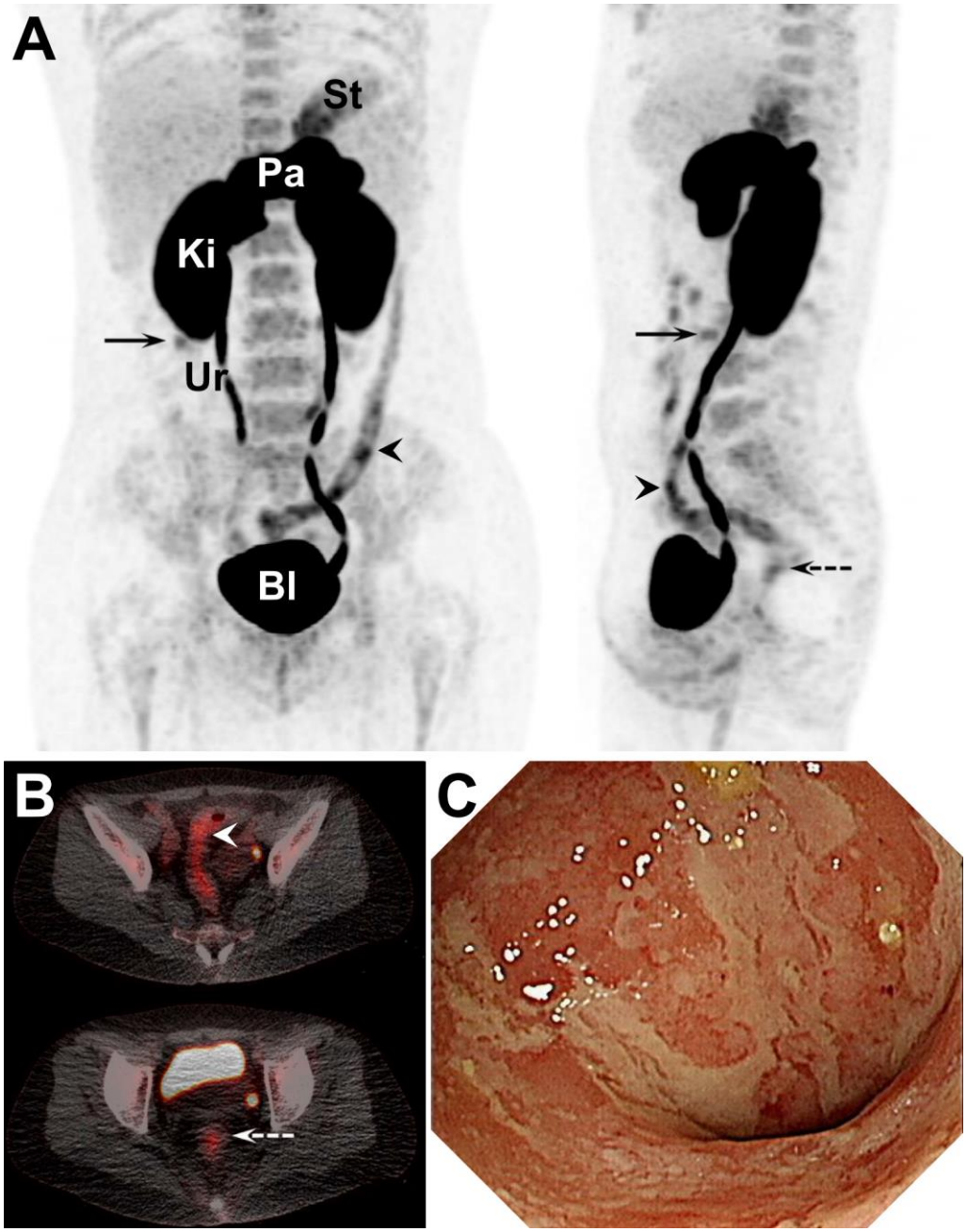

FIGURE 4. ^{18}F-FSPG PET/CT and endoscopic images of a 26-year-old woman with CD presented with abdominal pain and elevated C-reactive protein. Her Crohn's Disease Activity Index was 102.47. (A) Maximum intensity projection and (B) axial ^{18}F-FSPG PET show increased ^{18}F-FSPG uptake in the ileum (arrow), sigmoid and descending colon (arrowhead), and rectum (dotted arrow), which correlated well with endoscopic findings. The segmental CDEIS scores were 12 for the ascending colon, 0 for the transverse colon, 24 for the descending and sigmoid colon, and 23 for the rectum. The ileum was not assessed by colonoscopy. (C) Endoscopic image of the rectum shows geographic and superficial ulcers, exudates, and streaks of coagulated blood. St, stomach; Pa, pancreas; Ki, kidneys; Ur, ureter; and Bl, bladder.

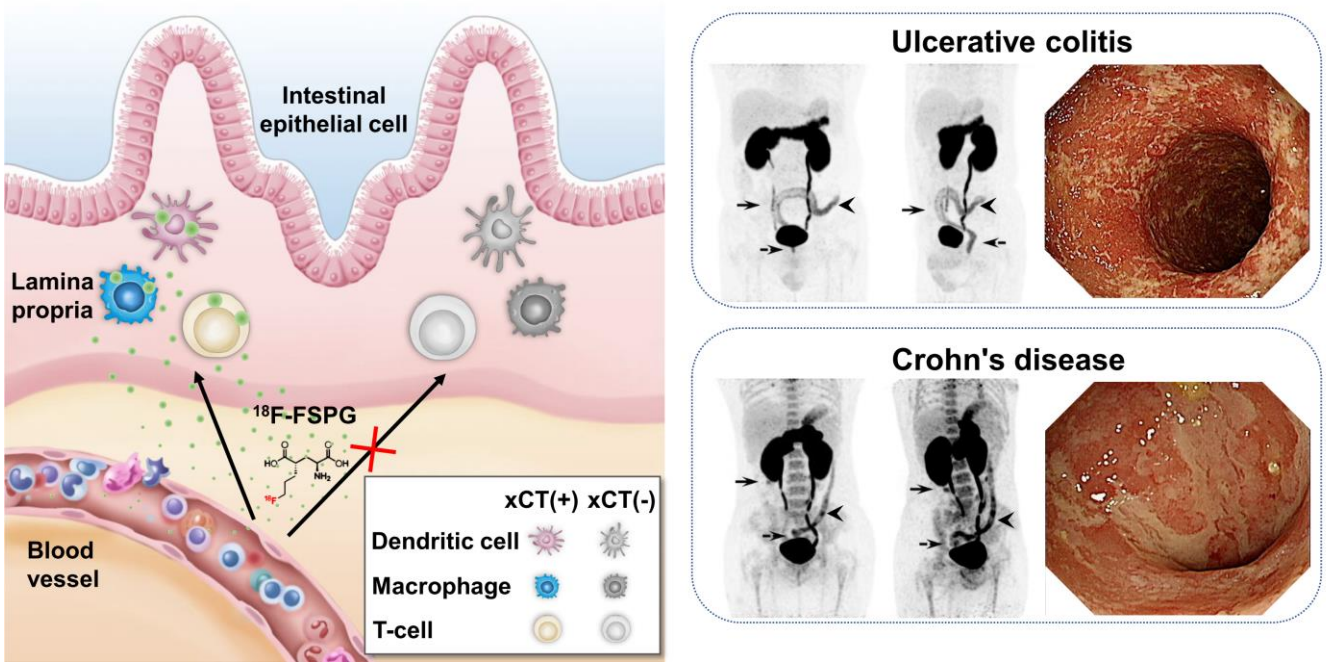

Graphical Abstract

Table 1 Demographic and clinical characteristics.

Characteristic	Ulcerative colitis	Crohn's disease
Asian (Korean)	10 (100%)	10 (100%)
Age, year	42 (22–56)	28 (21–34)
Male sex	6 (60%)	9 (90%)
Body mass index, kg/m^2	24.9 (17.1–36.9)	23.4 (18.7–30.0)
Smoking, Never smoker	6 (60%)	6 (60%)
Former smoker	3 (30%)	3 (30%)
Every day smoker	1 (10%)	1 (10%)
Disease duration, months	40.2 (5.2–91.0)	55.8 (50.3–99.4)
Partial Mayo score	2 (0–4)	NA
Remission, 0–2	7 (70%)	
Mildly active, 3–5	3 (30%)	
Crohn's Disease Activity Index	NA	91.89 (26.09–265.56)
Remission, <150		7 (70%)
Mildly active, 150–219		2 (20%)
Moderately active, 220–450		1 (10%)
Harvey-Bradshaw Index	NA	2 (1–12)
Remission, 0–4		8 (80%)
Mildly active, 5–7		1 (10%)
Moderately active, 8–16		1 (10%)
Hemoglobin, g/dL	14.2 (10.5–15.2)	14.2 (9.4–17.5)
White blood cell, $\times 10^3/\mu L$	7.7 (3.9–12.9)	6.9 (4.0–10.0)
Platelet, $\times 10^3/\mu L$	310 (233–405)	287 (223–521)

Erythrocyte sedimentation, mm/hr	15 (3–53)	17 (2–105)
C-reactive protein, mg/dL	0.11 (0.10–0.99)	0.43 (0.10–3.83)
Fecal calprotectin, μg/g	65.1 (30.0–721)	116 (36.1–2,810)
UCEIS	2 (0–5)	NA
CDEIS	NA	9.8 (0.8–28.5)

Data are reported as median (range) or number (%).NA = not applicable.

Supplemental Methods

Experimental IBD models, ^{18}F-FSPG PET imaging, and *ex vivo* analysis

Two experimental IBD models, induced by DSS in male Balb/c mice, aged 8–9 weeks and weighing 20–25g (Central Lab Animal, Inc., Seoul, Republic of Korea), and adoptive transfer of naïve T cells ($CD4^+CD45RB^{high}$) into male immunodeficient RAG2-knockout ($BALB/c\text{-}Rag2^{-/-}\gamma c^{-/-}$) mice, aged 8–12 weeks and weighing 25–35 g (Jackson Laboratory, Bar Harbor, ME, USA), were evaluated. The experimental unit was an individual animal, independently and nonrandomly allocated to a colitis or control group. Analysis of sample size showed that the minimum number of animals in each colitis or control group was 5 to 8, based on a significance level of $P < 0.05$ and a power of 80% for various differences in ^{18}F-FSPG uptake between IBD and control groups with a 15% or 20% coefficient of variation. Animals in the experimental IBD models were included in this study if they showed symptoms or signs of inflammation. Animals were excluded if they had lost >20% body weight during the study. These criteria were defined before the experiment. Researchers were aware of the group allocation during the conduct of the experiment and the assessment of clinical outcomes.

To induce colitis with dextran sulfate sodium (DSS), mice were administered 5% DSS (MP Biomedicals, Solon, OH, USA) in drinking water ad libitum for 7 days, followed by administration of normal drinking water. Body weight, rectal bleeding, and diarrhea were monitored daily. Clinical disease activity was determined as the average of weight loss scores (0, none; 1, 1–5%; 2, 5–10%; 3, 10–20%; 4, >20%), stool consistency scores (0, normal; 2, loose; 4, diarrhea), and bleeding scores (0, absence; 2, hematocrit positive; 4, gross bleeding).

To induce colitis by transfer of T cells, $CD4^+$ T cells were isolated from the spleens of wild-type BALB/c mice and purified using a $CD4^+$ T-cell isolation kit (Miltenyi Biotech, Bergisch Gladbach, Germany), followed by staining with anti-CD4 (RM4-5) and anti-CD45RB (16A) antibodies (BD Biosciences, Franklin Lakes, NJ, USA). $CD4^+CD45RB^{high}$ T-cells were sorted on a FACS Aria sorter (BD Biosciences). BALB/c background $Rag2^{-/-}\gamma c^{-/-}$ mice were injected i.p. with 5×10^5 $CD4^+CD45RB^{high}$ T cells. Body weight and diarrhea were monitored twice weekly. Clinical disease activity was determined as the average scores for weight loss (0, none; 2, 5–15%; 4, >15%) and stool consistency (0, normal; 2, mild symptoms; 4, severe diarrhea).

Mice were subjected to ^{18}F-FSPG PET imaging 1 week after DSS administration and 8–12 weeks after adoptive T-cell transfer using an animal PET/magnetic resonance imaging (PET/MRI) system (nanoScan PET/MRI, MEDISO, Ltd., Hungary). Static PET images were acquired 60 minutes after injection of 7.4 MBq (0.2 mCi) into the tail vein for 10 minutes. The standardized uptake value (SUV) was calculated using the formula: SUV = (tissue radioactivity in the volume of interest measured as MBq/cc × body weight) / injected radioactivity. The maximum value (SUVmax) in each mouse was chosen for analysis.

Immediately after PET imaging, the mice were sacrificed and the colon removed. The entire colon of each mouse was cut lengthwise and washed with phosphate-buffered saline, fixed in 4% paraformaldehyde, embedded in paraffin, and stained with Hematoxylin-Eosin. Pathologic scoring was performed in a blinded fashion. Mice with DSS-induced colitis were scored using a system based on three parameters: severity of inflammation (0, none; 1, slight; 2, moderate; 3, severe), extent of injury (0, none; 1, mucosa; 2, mucosa and submucosa; 3, transmural and loss of epithelium), and crypt damage (0, none; 1, basal one-third damaged; 2, basal two-thirds damaged;

3, only surface epithelium intact; 4, entire crypt and epithelium lost). The sum of the three scores was multiplied by a factor that reflected the percentage of tissue involvement (1, 0–25%; 2, 26–50%, 3, 51–75%; 4, 76–100%). Mice with IBD induced by T-cell transfer were subjected to pathologic scoring based on crypt architecture (0, normal; 1, irregular; 2, moderate crypt loss (10–50%); 3, severe crypt loss (50–90%); 4, small/medium sized ulcers (<10 crypt widths); 5, large ulcers (>10 crypt widths); crypt abscesses (0, normal; 1, 1–5; 2, 6–10; 3, >10); tissue damage (0, normal; 1, discrete lesions; 2, mucosal erosions; 3, extensive mucosal damage); inflammatory cell infiltration (0, occasional; 1, increased leukocytes in the lamina propria; 2, confluence of leukocytes extending to the submucosa; 3, transmural extension of inflammatory infiltrates); and goblet cell loss (0, normal to <10% loss; 1, 10–25% loss; 2, 25–50% loss; 3, >50% loss). The total pathological score was calculated by combining scores of the five parameters, with a maximum score of 17.

Immunohistochemical staining of mouse colon

Colon tissues were obtained from three mice each with DSS-induced and T-cell transfer-induced colitis and three corresponding control mice each, fixed in 4% paraformaldehyde and dehydrated in 15% and 30% sucrose solutions in phosphate-buffered saline. Tissues were embedded in optimal cutting temperature compound, and sections were fixed with acetone at -20°C for 5 minutes. Slides were blocked by incubation in phosphate-buffered saline (PBS) containing 1% bovine serum albumin for 1 hour at room temperature and stained with primary antibodies against x_C^-, glucose transporter, and cell surface markers overnight at 4°C. After washing in PBS, the tissue samples were incubated with secondary antibodies at room temperature for 1 hour and stained with 4′,6-

diamidino-2-phenylindole (Thermo, Waltham, MA, USA) for 2 minutes at room temperature, followed by mounting with PermaFluor mountant (Thermo). Images were captured on an LSM 710 confocal microscope (Carl Zeiss, Oberkochen, Germany). The primary antibodies were Alexa Fluor 488-conjugated anti-glucose transporter GLUT1 (EPR3915), rabbit anti-xCT (polyclonal), hamster anti-CD11c (HL3), PE-conjugated anti-CD3 (17A2), and PE-conjugated anti-F4/80 (CI:A3-1). Secondary antibodies were Alexa Fluor 568-conjugated goat anti-hamster IgG and Alexa Fluor 647 donkey anti-rabbit IgG. Antibodies were purchased from BD Biosciences, BioLegend (San Diego, CA, USA), Abcam (Cambridge, UK), and Novus Biologicals (Littleton, CO, USA).

Clinical study: Criteria for inclusion and exclusion

Inclusion criteria

A subject will be enrolled if s/he meets all of the following inclusion criteria:

- Subject is aged between 19 and 79 years, is male or female, and is of any race/ethnicity.
- Subject has had UC or CD diagnosed by clinical, endoscopic, and histologic evidence for at least 3 months prior to screening.
- Subject has symptoms suggestive of active disease at the time of enrollment.
- Subject is scheduled to undergo sigmoidoscopy or colonoscopy for UC or CD within 7 days prior to or after the planned ^{18}F-FSPG administration.

Exclusion criteria

A subject is to be excluded from the study if s/he does not fulfill all of the inclusion criteria or displays any of the following exclusion criteria:

- Subject or his/her legally acceptable representative does not provide written informed consent.
- Subject displays clinical signs of ischemic colitis or has evidence of pathogenic bowel infection.
- Subject has been diagnosed as having unclassified inflammatory bowel disease.
- Subject has been treated with sulfasalazine or intravenous corticosteroids within the previous 4 weeks prior to the planned ^{18}F-FSPG administration.
- Dose escalation of current IBD drugs or start of a new oral aminosalicylate, corticosteroid, immunomodulator, biologics, antibiotics, probiotics, or topical preparations is scheduled from the time of study enrollment to the scheduled sigmoidoscopy or colonoscopy, or 24 hours after ^{18}F-FSPG administration. Dose escalation or starting a new antidiarrheal and/or analgesic drug is allowed.
- Female subject is pregnant or nursing. The possibility of pregnancy is excluded if 1) a woman is physiologically post-menopausal (cessation of menses for more than 2 years); 2) a woman is surgically sterile (has had a documented bilateral oophorectomy and/or documented hysterectomy; or 3) a woman of childbearing potential is negative on a serum or urine pregnancy test performed within 24 hours immediately prior to administration of ^{18}F-FSPG; the latter women are advised to utilize contraceptive measures during participation in this study.

- Subject has concurrent severe and/or uncontrolled and/or unstable medical disease (e.g., congestive heart failure, acute myocardial infarction, severe pulmonary disease, chronic renal or hepatic disease) that, in the opinion of the investigator, could compromise participation in the study.
- Subject is a relative or student of the investigator, or is otherwise dependent on the investigator.
- Subject has received any investigational drugs or devices within 4 weeks prior to study enrollment.
- Subject was previously included in this study.
- Subject has any other condition or personal circumstances that might make a collection of complete data difficult or impossible, in the judgment of the investigator.
- Subject is allergic to hyoscine or any of the ingredients of hyoscine butylbromide, or has myasthenia gravis, megacolon, closed-angle glaucoma, or obstructive prostatic hypertrophy.

^{18}F-FSPG PET/CT imaging of patients: safety and interpretation

The safety of ^{18}F-FSPG was assessed based on laboratory parameters (serum chemistry), vital functions (blood pressure, heart rate, and body temperature), and physical examinations at baseline and 3 hours after ^{18}F-FSPG injection. Follow-up safety information was collected again at 24 hours. Adverse events were continuously monitored from patient enrollment until the last ^{18}F-FSPG-related adverse events were resolved, or up to a maximum of 28 days after the follow-up visit.

Based on the knowledge of ^{18}F-FSPG biodistribution (*1,2*), the intensity of ^{18}F-FSPG uptake was classified according to a 5-point scale, with 1 indicating no uptake above background; 2 indicating uptake less than or equal to a blood pool; 3 indicating uptake greater than the blood pool but less than or equal to that of the liver; 4 indicating moderately higher uptake compared with the liver; and 5 indicating markedly increased uptake compared with the liver. The location and intensity of ^{18}F-FSPG activity were assessed in the rectum, sigmoid colon, descending colon, transverse colon, and ascending colon of patients with UC; and in the rectum, sigmoid and descending colon, transverse colon, ascending colon, and ileum of patients with CD. The maximum ^{18}F-FSPG score was the highest value among segmental scores, with a score ≥4 considered positive for active disease. In our retrospective analysis approved by the institutional review board of Asan Medical Center (2019-0052), only 4 (2.2%) of 180 bowel segments from the subjects with no history of IBD had scores ≥4 (*1,2*). For quantitative analysis, volumes of interest were drawn on each bowel segment, using the combined CT data for anatomical localization.

Assessment of clinical and pathological assessment of disease activity

Clinical disease activity was assessed in patients with UC using the partial Mayo score, and patients with CD using the Crohn's Disease Activity Index and Harvey-Bradshaw Index (*3*). Bowel segments were histologically evaluated by an experienced pathologist, who was blinded to the results of ^{18}F-FSPG PET/CT, using the Robarts Histopathological Index for patients with UC (*3*) and the Colonic and Ileal Global Histological Disease Activity Score for patients with CD, with the latter modified by excluding the number of biopsies.

Immunohistochemical staining of human xCT, GLUT1, and cell surface markers

Multiplex immunofluorescence staining was performed using a Leica Bond Rx™ Automated Stainer (Leica Biosystems, Newcastle, U.K), as described previously (*4*). Tissue sections were incubated with primary antibodies, followed by a secondary polymer-horseradish peroxidase-bound antibody (Polymer HRP MS + Rb, ARH1001EA; Akoya Biosciences, Marlborough, MA, USA). Images of multiplex immunofluorescence staining were captured using the Vectra Polaris Automated Quantitative Pathology Imaging System (Akoya Biosciences). A region of interest was placed on the abnormal mucosa that revealed abnormal features of inflammatory bowel disease, as determined by an experienced pathologist. Immune cell populations positive for xCT, GLUT1, and cell surface markers were characterized and quantified by tissue segmentation, cell segmentation, and phenotyping, as determined by inForm version 2.2 software (Akoya Biosciences). Batch analysis was performed on each tissue's selected region of interest using the

same algorithm designed for representative images. The number of cells with each phenotype was calculated using RStudio version 1.3.1073 software and classified using TIBCO Spotfire™ (TIBCO Software, Palo Alto, CA, USA). The numbers of labeled cells per mm^2 were quantified.

Statistical analysis

Continuous variables are reported as median and range, whereas categorical variables are reported as numbers (%). Quantitative variables were compared by Mann–Whitney U-tests. Associations between variables were assessed by nonparametric Spearman rank correlation coefficient analysis. The inter-reader variability of visual assessment of ^{18}F-FSPG accumulation was assessed using kappa statistics with 95% confidence intervals. All statistical analyses were conducted using IBM SPSS Statistics for Windows (version 21; IBM Company, Armonk, NY), with two-sided *P*-values <0.05 considered statistically significant.

Supplemental Figures

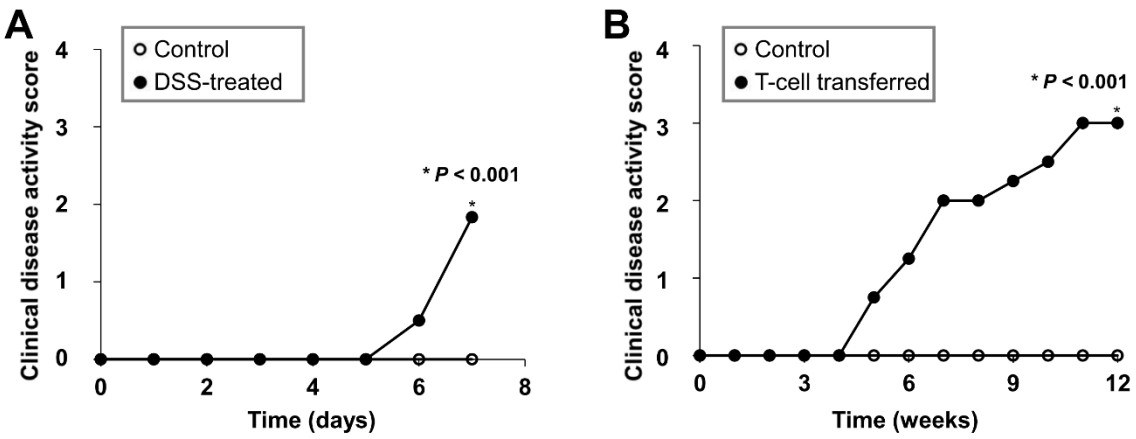

Supplemental Figure 1. Median clinical disease activity scores of mouse models of IBD induced by (A) DSS treatment and (B) adoptive transfer of T cells, as well as their respective controls.

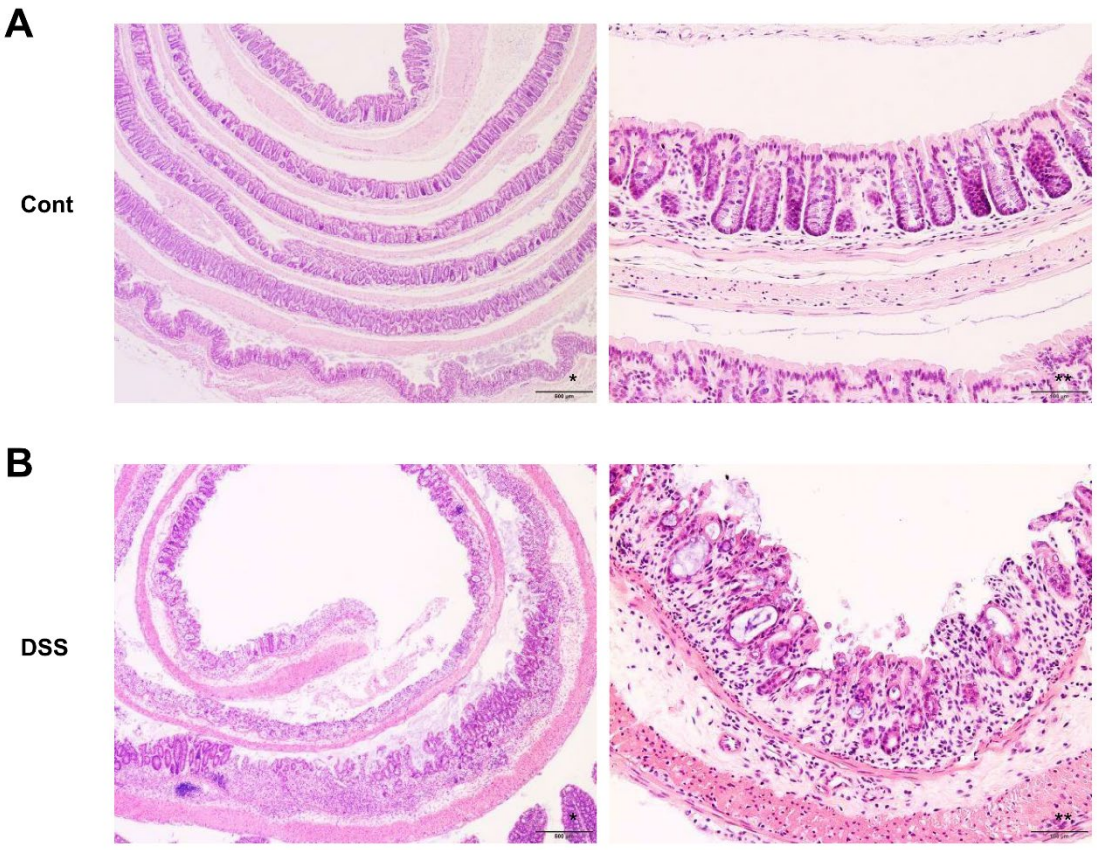

Supplemental Figure 2. Representative images of hematoxylin–eosin-stained colonic sections of (A) normal control and (B) DSS-treated Balb/c mice. Colon epithelium was severely damaged and infiltrated with inflammatory cells after DSS treatment. Images were viewed using an Olympus BX-53 microscope (Olympus, Japan). Scale bar = 500 μm (*) and 100 μm (**).

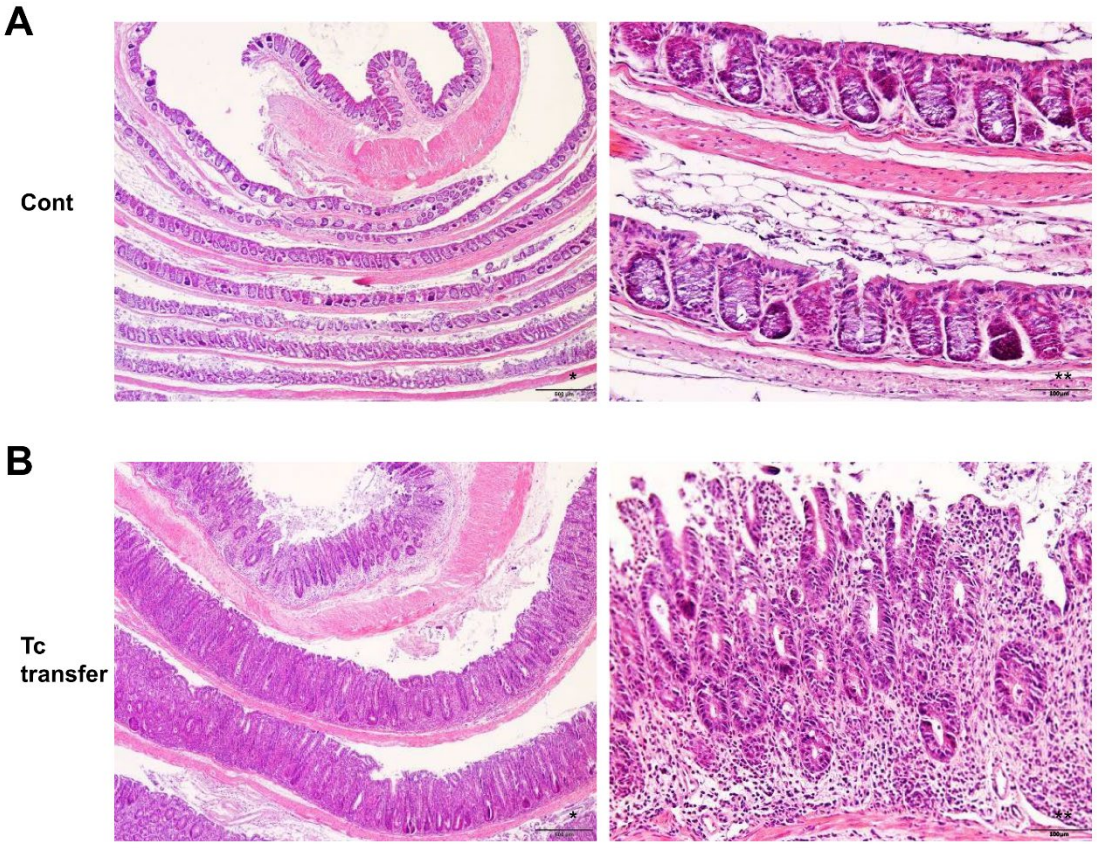

Supplemental Figure 3. Representative images of hematoxylin–eosin-stained colonic sections of (A) control and (B) adoptive T-cell–transferred BALB/c-Rag2$^{-/-}$γc$^{-/-}$ mice (B). T-cell–transferred mice exhibit markedly elongated crypts, a reduced number of goblet cells, and increased infiltration of inflammatory cells in the lamina propria. Images were viewed using an Olympus BX-53 microscope (Olympus, Japan). Scale bar = 500 μm (*) and 100 μm (**).

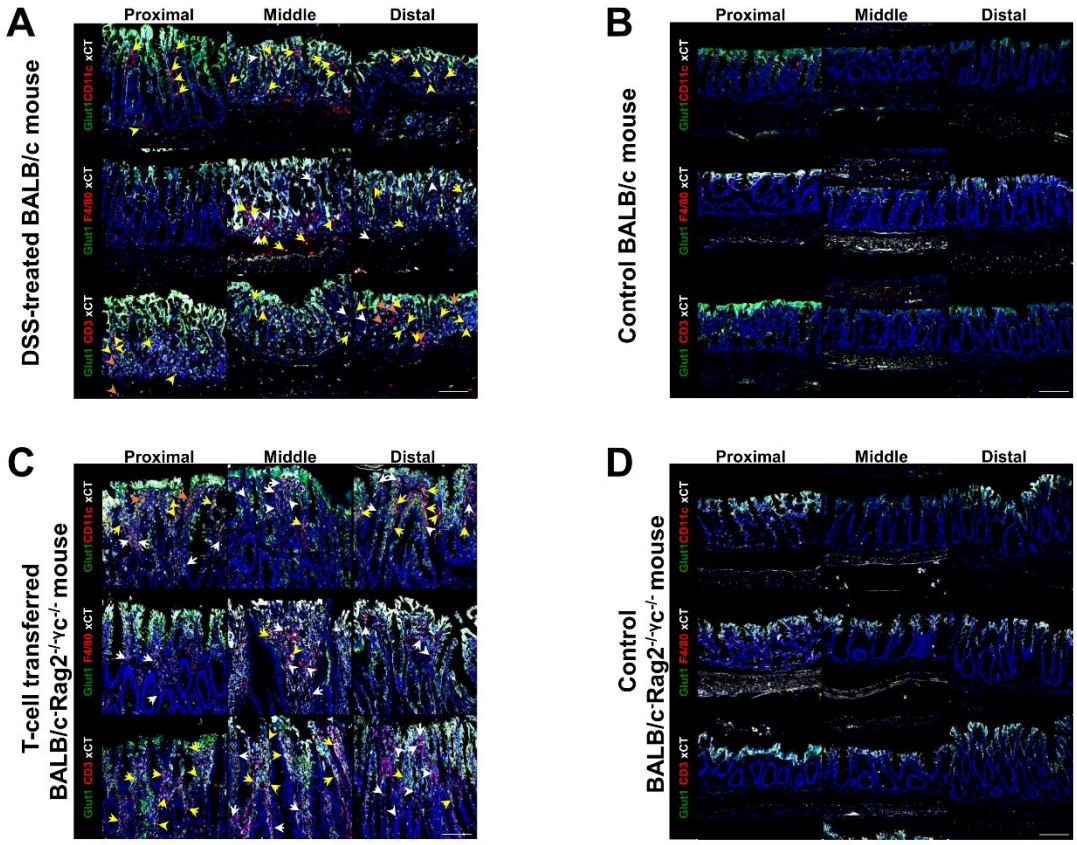

Supplemental Figure 4. Confocal microscopic images of colonic sections from experimental IBD and normal control mice. Representative xCT (white), Glut1 (green), and cell surface marker (red) immunohistochemical images of (A) DSS-treated and (B) control BalB/c mice, and of (C) adoptive T-cell–transferred and (D) control BALB/c-Rag2$^{-/-}$γc$^{-/-}$ mice. The first column shows images of the proximal colons, followed by the middle and distal colons. The intestinal epithelia of both experimental colitis and control mice were positive for xCT and Glut1 staining. However, increased numbers of xCT or Glut1 positive inflammatory cells (CD11c^{+} dendritic cells, F4/80^{+} macrophages, and CD3^{+} T cells) were observed in the lamina propria of (A) DSS-treated and (C) adoptive T-cell–transferred mice than in their respective controls. Yellow, orange, and white arrows

indicate xCT/Glut1/cell surface marker-positive, Glut1/cell surface marker-positive, and xCT/cell surface marker-positive cells, respectively. Images were viewed using an LSM 710 confocal microscope (Carl Zeiss, Oberkochen, Germany). Scale bar = 100 μm.

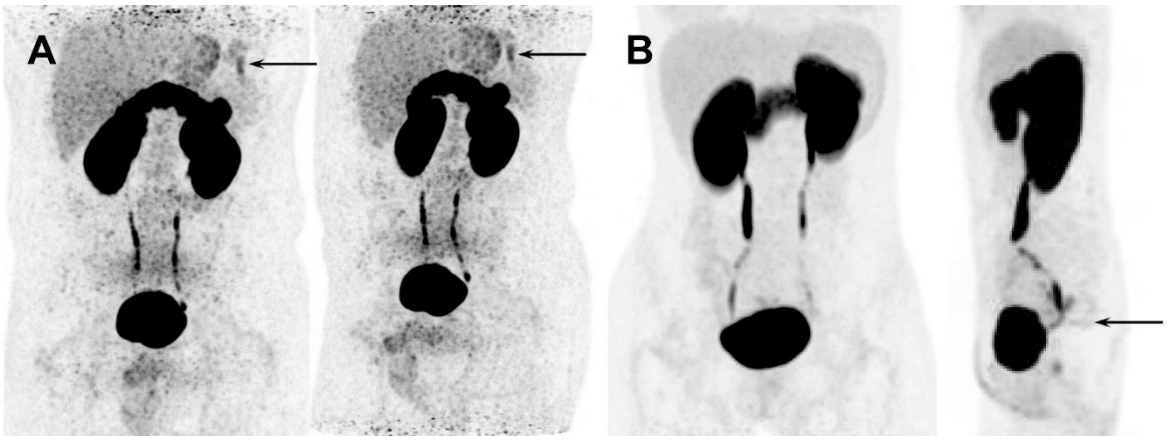

Supplemental Figure 5. False-negative ^{18}F-FSPG PET maximum intensity projection images of patients with UC. (A) Anterior and left anterior oblique images of a 32-year-old man with UC, showing a small focus of ^{18}F-FSPG uptake along the transverse colon (arrow), which was visually graded as a score of 3. The corresponding UCEIS was 4. (B) Anterior and lateral images of a 22-year-old woman with UC, showing mild ^{18}F-FSPG uptake in the rectum (arrow), which was visually interpreted as a score of 3. The corresponding UCEIS was 2.

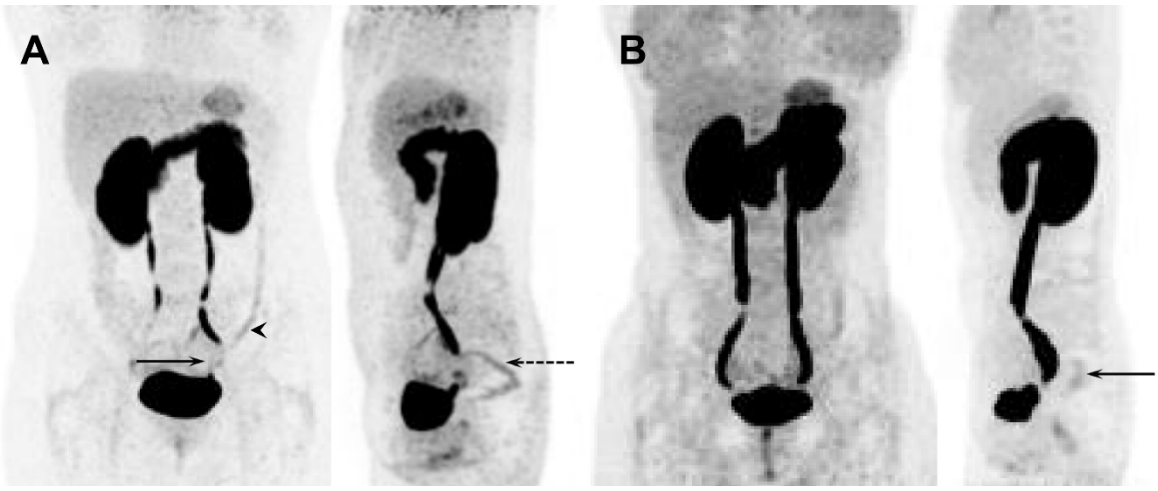

Supplemental Figure 6. False-positive ^{18}F-FSPG PET maximum intensity projection images of patients with UC. (A) Anterior and lateral images of a 41-year-old woman with UC, showing mild ^{18}F-FSPG uptake along the descending colon (arrowhead), the sigmoid colon (arrow), and the rectum (dotted arrow), all of which were visually interpreted as moderately increased intensity compared with the liver (score 4). The UCEIS was 0. (B) Anterior and lateral images of a 24-year-old woman with UC, showing mild ^{18}F-FSPG uptake in the rectum (arrow), which was also visually assessed as moderately increased intensity compared with the liver (score 4). The corresponding UCEIS was 0.

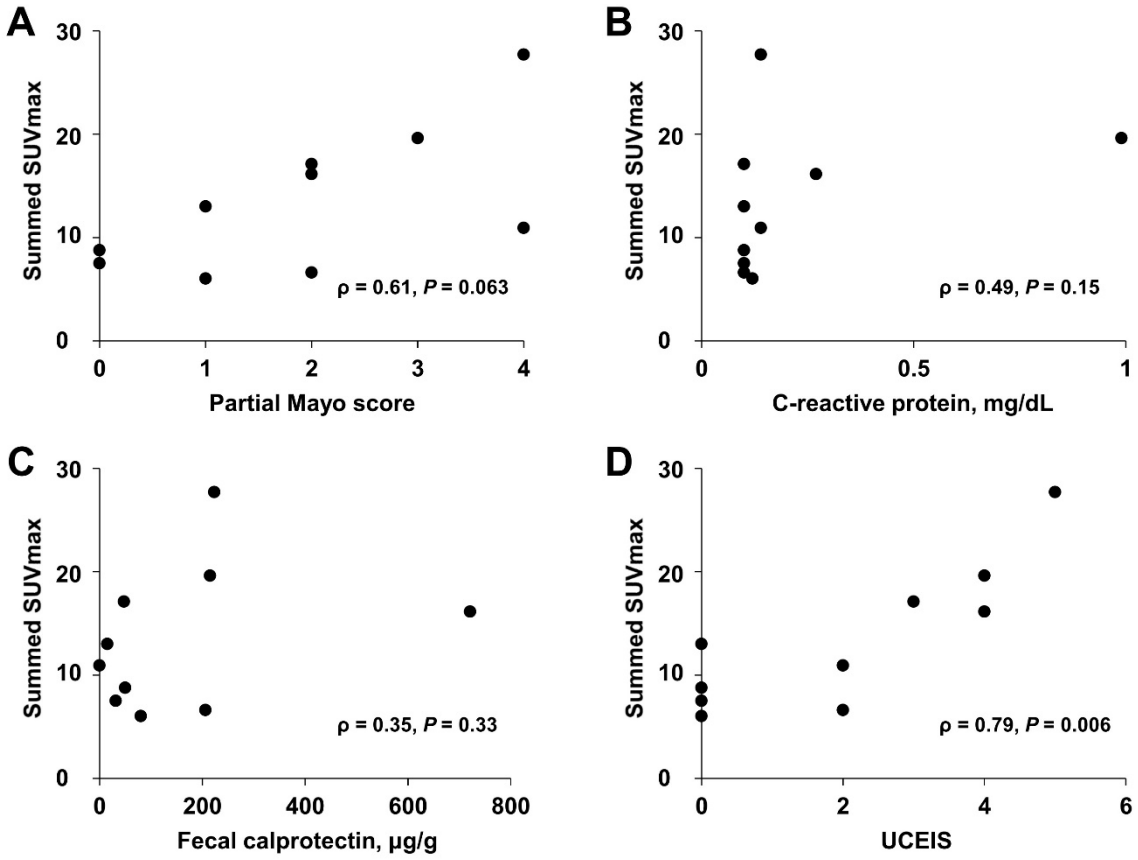

Supplemental Figure 7. Association between ^{18}F-FSPG SUVmax and markers of disease activity in patients with UC (n = 10).

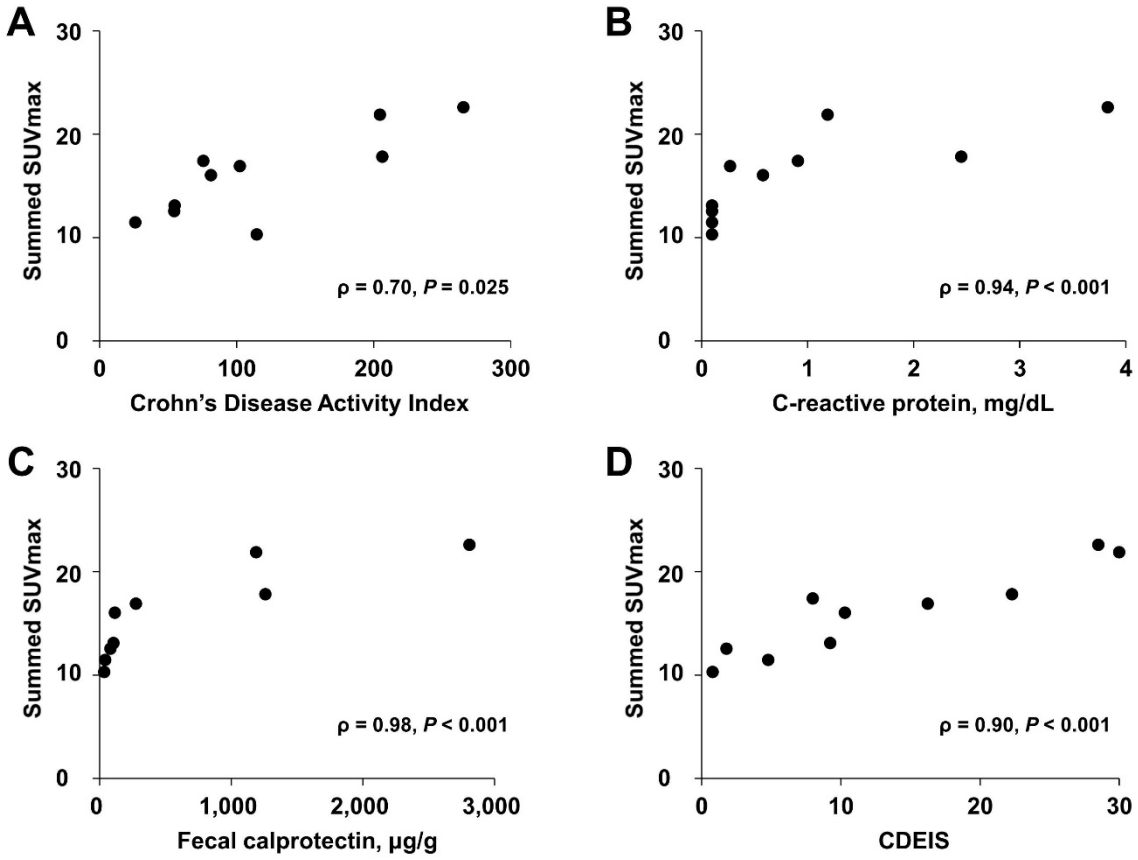

Supplemental Figure 8. Association between 18F-FSPG SUVmax and markers of disease activity in patients with CD (n = 10).

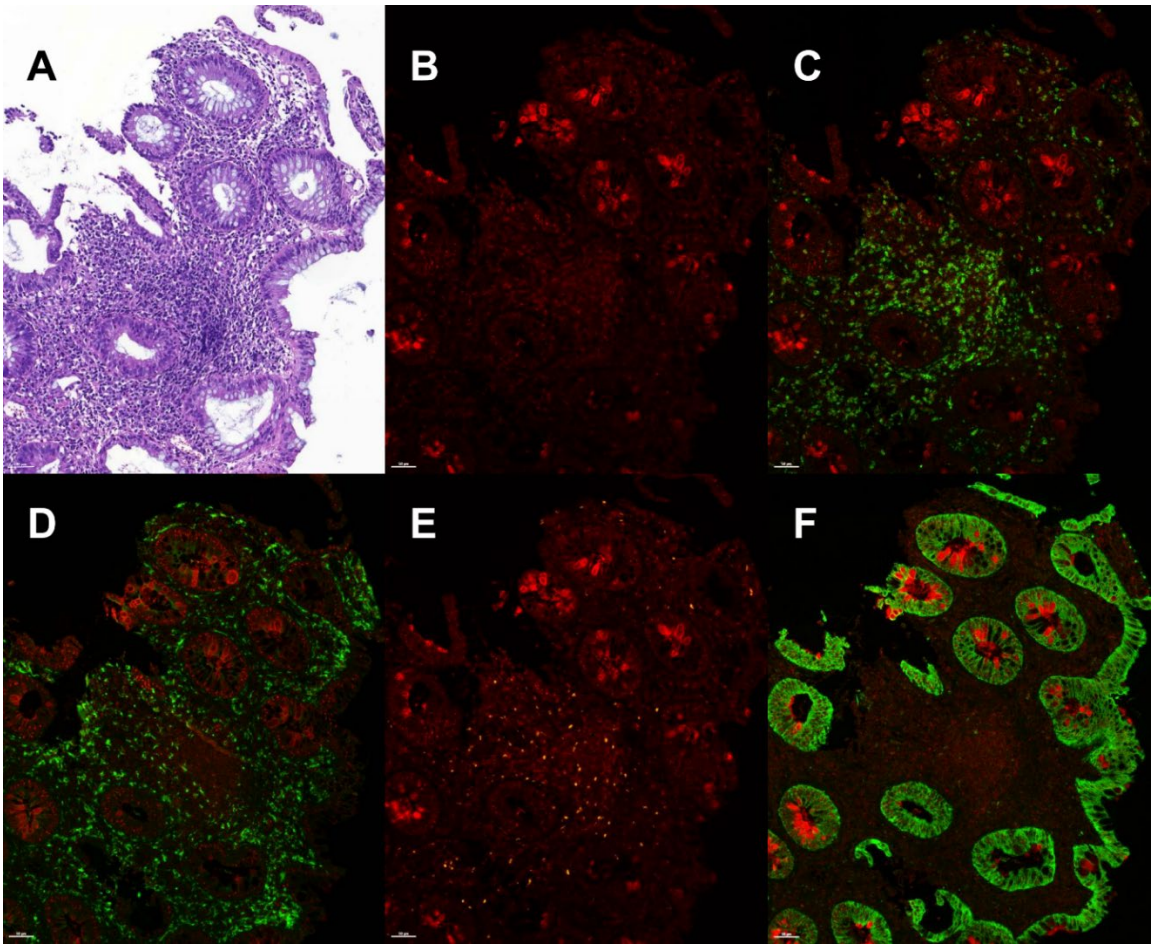

Supplemental Figure 9. Immunohistochemical staining for xCT and cell surface markers in patients with active UC. (A) Hematoxylin–eosin-stained colonic tissue and (B) immunohistochemical staining showing positive xCT expression in the epithelium and lamina propria. (C-E) Coexpression of xCT and the cell surface markers (C) CD68, (D) CD3, and (E) CD66b in the lamina propria. (F) Expression of xCT in cytokeratin-positive epithelial cells is limited to the luminal aspect of the mucosa. Color correspondence: Red = xCT; Orange = CD66b; Green = CD68, CD3, or cytokeratin. Slides were digitized using a Panoramic SCAN digital slide scanner (3 DHISTECH, Budapest, Hungary).

Scale bar = 50 μm.

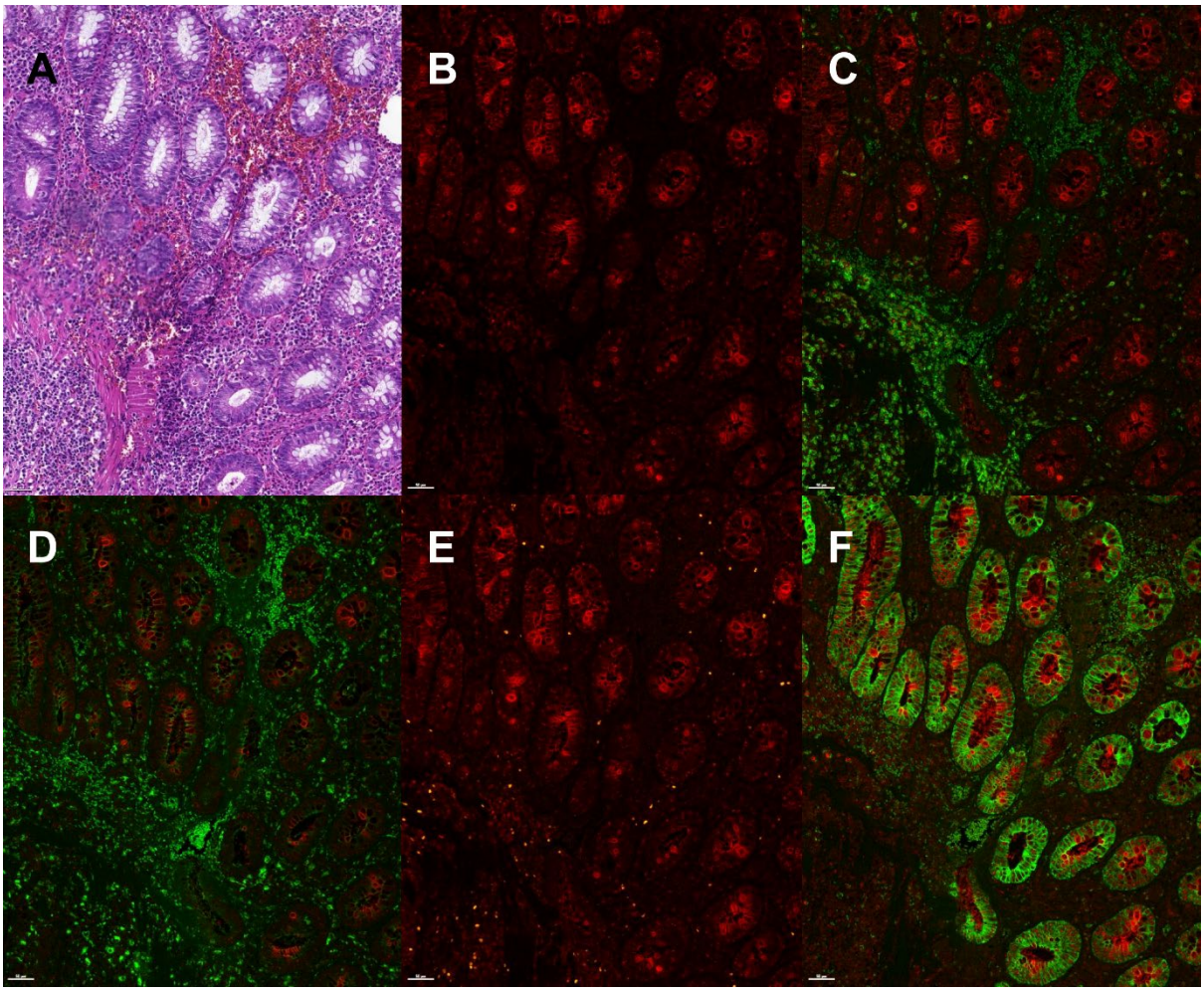

Supplemental Figure 10. Immunohistochemical staining for xCT and cell surface markers in patients with active CD. (A) Hematoxylin–eosin-stained colonic tissue and (B) immunohistochemical staining show positive xCT expression in the epithelium and lamina propria. (C-E) Coexpression of xCT and the cell surface markers (C) CD68, (D) CD3, and (E) CD6bb in the lamina propria. (F) Expression of xCT in cytokeratin-positive epithelial cells is limited to the luminal aspect of the mucosa. Color correspondence: Red = xCT; Orange = CD66b; Green = CD68, CD3, or cytokeratin. Scale bar = 50 μm.

Supplemental Tables

Supplemental Table 1. List of primary antibodies used for immunohistochemical staining of xCT and cell surface markers.

[a]Primary antibody	Clone (Supplier)	Antibody titer
xCT	Polyclonal (NB300-318, Novus Biologicals)	1:250
GLUT1	Polyclonal (ab15309, Abcam)	1:200
CD68	PG-M1 (M0876, Dako Products, Agilent)	1:100
CD3	2GV6 (790-4341, Ventana)	1:200
CD66b	G10F5 (NB100-77808, Novus Biologicals)	1:500
Cytokeratin	AE-1/AE-3 (NBP2-29429, Novus Biologicals)	1:300

[a]Tyrimide signal amplification: Opal 520 for CD68, CD3, and cytokeratin; Opal 620 for CD66b; Opal 650 and 690 for xCT; Opal 780 for GLUT1.

Supplemental Table 2. Validity of ^{18}F-FSPG PET/CT for diagnosis of active ulcerative colitis.

	Patients with active ulcerative colitis		
^{18}F-FSPG PET/CT	**Positive**	**Negative**	**Total**
Positive	4	2	6
Negative	2	2	4
Total	6	4	10
	Bowel segments with active ulcerative colitis		
^{18}F-FSPG PET/CT	**Positive**	**Negative**	**Total**
Positive	9	5	14
Negative	3	30	33
Total	12	35	47

Supplemental Table 3. Validity of ^{18}F-FSPG PET/CT for diagnosis of active Crohn's disease.

	Patients with active Crohn's disease		
^{18}F-FSPG PET/CT	**Positive**	**Negative**	**Total**
Positive	8	0	8
Negative	0	2	2
Total	8	2	10
	Bowel segments with active Crohn's disease		
^{18}F-FSPG PET/CT	**Positive**	**Negative**	**Total**
Positive	17	1	18
Negative	7	16	23
Total	24	17	41

Supplemental Table 4. Immunohistochemical determination of the expression of xCT and cell surface markers and their association with UCEIS and quantitative ^{18}F-FSPG uptake in 22 bowel segments in patients with UC.

Immunohistochemistry		**Cell number / mm^2**		**UCEIS**		**SUV**	
Cell	**xCT**	**Median**	**Range**	**ρ**	***P*-value**	**ρ**	***P*-value**
CD68+	xCT$^+$	153	9–594	0.54	0.010	0.57	0.006
	xCT$^-$	51	5–309	0.33	0.129	0.29	0.191
	GLUT1$^+$	5	0–183	0.30	0.183	0.13	0.567
CD3+	xCT$^+$	281	30–8705	0.70	<0.001	0.69	<0.001
	xCT$^-$	521	58–1480	0.17	0.442	0.22	0.334
	GLUT1$^+$	37	0–814	0.16	0.477	0.07	0.747
CD66b+	xCT$^+$	93	0–1532	0.35	0.111	0.43	0.048
	xCT$^-$	67	0–2544	0.59	0.004	0.67	0.001
	GLUT1$^+$	17	0–429	0.22	0.330	0.24	0.290
CK+	xCT$^+$	2430	308–4103	–0.63	0.002	–0.61	0.002
	xCT$^-$	142	52–1067	−0.00	0.993	−0.05	0.832
	GLUT1$^+$	0	0–71	0.06	0.794	−0.05	0.829

Supplemental Table 5. Immunohistochemical determination of the expression of xCT and cell surface markers and their association with CDEIS and quantitative ^{18}F-FSPG uptake in seven bowel segments in patients with CD.

Immunohistochemistry		**Cell number / mm^2**		**CDEIS**		**SUVmax**	
Cell	**xCT**	**Median**	**Range**	**ρ**	***P*-value**	**ρ**	***P*-value**
CD68+	xCT$^+$	111	24–541	0.95	0.001	0.21	0.645
	xCT$^-$	121	46–298	−0.44	0.328	0.07	0.879
	GLUT1$^+$	10	0–25	0.18	0.694	0.14	0.758
CD3+	xCT$^+$	570	153–1229	0.35	0.448	0.46	0.294
	xCT$^-$	414	47–1428	0.06	0.908	0.54	0.215
	GLUT1$^+$	14	6–52	0.66	0.111	−0.21	0.645
CD66b+	xCT$^+$	50	0–852	0.68	0.093	0.22	0.632
	xCT$^-$	311	0–736	0.13	0.786	−0.11	0.819
	GLUT1$^+$	43	0–201	0.16	0.738	−0.02	0.969
CK+	xCT$^+$	2992	2447–4769	0.20	0.667	0.54	0.215
	xCT$^-$	596	249-1335	−0.49	0.263	0.11	0.819
	GLUT1$^+$	6	0–164	−0.27	0.564	0.13	0.788

Supplemental References

1. Baek S, Mueller A, Lim YS, et al. (4S)-4-(3-18F-fluoropropyl)-L-glutamate for imaging of xC transporter activity in hepatocellular carcinoma using PET: preclinical and exploratory clinical studies. *J Nucl Med.* 2013;54:117-123.

2. Chae SY, Choi CM, Shim TS, et al. Exploratory clinical investigation of (4S)-4-(3-18F-fluoropropyl)-L-glutamate PET of inflammatory and infectious lesions. *J Nucl Med.* 2016;57:67-69.

3. Walsh AJ, Bryant RV, Travis SP. Current best practice for disease activity assessment in IBD. *Nat Rev Gastroenterol Hepatol.* 2016;13:567-579.

4. Ahn J, Jin M, Song E, et al. Immune profiling of advanced thyroid cancers using fluorescent multiplex immunohistochemistry. *Thyroid.* 2021;31:61-67.